Coherent population transfer in multilevel systems with magnetic sublevels. I. Numerical studies

B. W. Shore,* J. Martin, M. P. Fewell,† and K. Bergmann
Fachbereich Physik der Universität Kaiserslautern, 67653 Kaiserslautern, Germany
(Received 23 September 1994)

The technique of stimulated Raman adiabatic passage has become an established procedure for producing complete population inversion in atoms or molecules via application of Stokes and pump pulses in a counterintuitive sequence. We discuss here some of the new and important phenomena that arise when some of the states involved have nonzero angular momentum, the field polarization directions have no simplifying symmetries, and Zeeman splitting lifts the magnetic sublevel degeneracy. We consider the effects of the linkage structure of the Hamiltonian, the effects of various polarization directions, and the effects of various choices for carrier frequencies, as expressed by detunings from single-photon resonance. In particular, we consider an example with angular momentum $J = 0 \Leftrightarrow J = 1 \Leftrightarrow J = 2$ in which nine magnetic sublevels occur. We show that under suitable conditions it is possible, simply through the appropriate tuning of pump and Stokes carrier frequencies, to place the entire population into any specified single magnetic sublevel.

PACS number(s): 42.50.Hz, 42.50.Rh, 42.65.Dr

I. INTRODUCTION

A. Basic stimulated Raman adiabatic passage

There is much contemporary interest in techniques that can control translational and internal degrees of freedom of atoms or molecules through interactions with laser radiation [1–11]. Applications include detailed studies of collision dynamics [12–14], spectroscopy [15], atomic interferometers [8], and even cavity quantum electrodynamics [16].

Among the techniques in use for population transfer are optical pumping, Franck-Condon pumping for molecules [17,18], and stimulated emission pumping [19,20]. Techniques based upon adiabatic passage [3,21,22], via controlled temporal variation of elements of the Hamiltonian, offer possibilities for producing complete population transfer. The adiabatic variation can occur either in the diagonal elements, as changes in differences between Bohr frequencies and laser frequencies, or in the off-diagonal elements, through pulsed variation of radiation intensity.

A potentially valuable example of adiabatic population manipulation, termed stimulated Raman adiabatic passage (STIRAP) [3], recently reviewed [23], has been discussed theoretically [24–39] and demonstrated experimentally [3,10,40]. In its most elementary form, the STIRAP process takes place in a nondegenerate three-state system (an initially populated ground state 1, a final state 3, and an intermediate state 2), coupled to two pulsed radiation fields (termed pump and Stokes fields) in a conventional Raman configuration (sometimes termed a Λ system, as distinct from a V or ladder arrangement of the three energies). The process employs a counterintuitive pulse sequence [3,35] starting with application of the Stokes pulse (connecting states 2 and 3) and ending with application of the pump pulse (connecting states 1 and 2). By enforcing adiabatic evolution of a dressed state as the state vector, together with continued two-photon resonance, one can force complete population transfer between state 1 and state 3. If two-photon resonance is maintained, then the resulting complete transfer is insensitive to the pump or the Stokes detunings from respective single-photon resonance and at no time does appreciable population reside in intermediate state 2.

A number of extensions of the basic three-state STIRAP procedure have been discussed, including the effects of pulse bandwidth [33], the presence of multiple intermediate states or multiple final states [28], and the use of four- or five-state sequences [37,38,41]. Such theoretical work, together with recent experimental confirmations, suggests that the mechanism of adiabatic passage via counterintuitive pulse sequences has broad applicability beyond the original three-state system.

The present paper examines a different and important multilevel aspect of the STIRAP procedure, involving the magnetic sublevel structure that accompanies rotational degeneracy. Our objective is to find procedures that will allow selective excitation into different magnetic sublevels selected simply by tuning the laser frequencies. We illustrate the possibilities by examining in detail a particular case, excitation of the sequence $J = 0 \Leftrightarrow J = 1 \Leftrightarrow J = 2$ by linearly polarized lasers. The example, observable in metastable neon, is sufficiently general to illustrate a number of important considerations and problems that have hitherto escaped notice.

*Permanent address: Lawrence Livermore National Laboratory, Livermore, CA 94550.
†Permanent address: Department of Physics, University of New England, Armidale, New South Wales 2351, Australia.

B. STIRAP with sublevels

The simple picture of population transfer between two quantum states via an intermediate state, as is the case in traditional STIRAP, requires modification when the atom or molecule possesses nonzero angular momentum. A quantum state having angular momentum J has $2J+1$ magnetic sublevels that, in the absence of external fields, are degenerate in energy. In such a system population control includes control of alignment or orientation or, for most detailed control, transfer of population into a single magnetic sublevel.

Optical pumping techniques have been used both to remove population from a sublevel [11,42–45] and to transfer all population into one sublevel [11]. However, although this technique can place population entirely into individual sublevels with $M = 0$ or $\pm J$, it does not permit transfer into other single sublevels. It is therefore of interest to ask whether STIRAP can produce selective transfer into an arbitrary sublevel.

The possibility of extending the STIRAP concept, which has already been used to align atomic angular momentum [40], to excitation involving magnetic sublevels has attracted some attention [46–48]. In the simplest proposals, optical selection rules, together with appropriate choices of pump and Stokes polarizations, reduce the full set of magnetic sublevels to smaller sets of uncoupled triads [40]. It is then possible to populate selectively a single final sublevel by utilizing selection rules in concert with various optical devices that produce particular polarizations of the radiation (see the diagrams below). For such cases the traditional STIRAP is possible when the appropriate two-photon resonance tuning holds and the usual adiabatic conditions are met [3]. As noted below, it is possible to introduce this simplification with or without Zeeman shifts induced by a static magnetic field.

In some of these applications [8,46,47], simple selection rules act to convert the sublevel system into a simple multilevel ladder of the sort discussed previously. Under the most general conditions of pump and Stokes polarizations (e.g., polarizations not collinear) the excitation linkages do not separate into smaller sets of independent pathways. Such situations raise the interesting possibility that, when the linkages connect more than three states into a pattern that includes more than one final sublevel, then it may be possible to populate a single selected magnetic sublevel simply by suitable tuning of the laser carrier frequencies to match a resonance condition with one of the Zeeman-shifted sublevels. In such cases the radiation polarization remains fixed (but the pump and the Stoke polarizations are not collinear) and the Zeeman-shifting static magnetic field remains constant, while either the pump or the Stoke field is tuned in frequency so as to establish the appropriate two-photon resonance condition.

In this paper we will discuss a number of problems that arise when there are magnetic sublevels, separated in energy by a Zeeman shift. We shall present results of modeling pulsed excitation sequences, using both the Schrödinger equation and a density matrix equation. In a companion paper [49] we present an algebraic analysis of some of the features that are of particular importance for successful population transfer.

C. Population dynamics: Numerical integration

Population transfer that occurs during a much shorter time interval than the lifetime for spontaneous emission from intermediate states can be satisfactorily described by the time-dependent Schrödinger equation

$$\hbar\frac{\partial}{\partial t}\Psi(t) = -i\hat{H}(t)\Psi(t). \tag{1.1}$$

Although this equation is adequate for treating ideal STIRAP, because no population occurs in radiatively decaying states, a more realistic model of general experiments (allowing some population to be lost and other population to be recycled by optical pumping) requires the use of a density matrix $\hat{\rho}(t)$, through the solution to the generalized Bloch equation (see [11], p. 354)

$$\hbar\frac{\partial}{\partial t}\hat{\rho}(t) = -i[\hat{H}(t)\hat{\rho}(t) - \hat{\rho}(t)\hat{H}(t)] - \hbar\hat{\Gamma}\hat{\rho}(t), \tag{1.2}$$

where $\hat{\Gamma}$ describes the effects of spontaneous emission. The nonzero elements of $\hat{\Gamma}\hat{\rho}$ are expressible in terms of spontaneous emission rates A_{ij} between levels i and j,

$$[\hat{\Gamma}\hat{\rho}(t)]_{ij} = \rho_{ij}(t)\sum_k \frac{1}{2}(A_{ik} + A_{jk}) - \delta_{ij}\sum_k \rho_{kk}(t)A_{ki}. \tag{1.3}$$

We will present results of computer simulation for both the Schrödinger equation and the more elaborate equations for the density matrix. For the latter computations we included spontaneous emission with rates appropriate to the STIRAP transitions between the two metastable levels $^3P_0$ and $^3P_2$ of neon, via the intermediate level $^3P_1$. The numerical solutions to the coupled first-order ordinary differential equations [9 equations for the Schrödinger equation and, because of symmetries of the rotating-wave approximation (RWA) Hamiltonian, 45 equations for the density matrix] were obtained with an eighth-order Runge-Kutta algorithm with adaptive step-size control.

In what follows we will describe the RWA Hamiltonian of interest, taking into account the different orientations of the polarization directions of the field. We will discuss the linkage patterns that result from various polarization choices. We will discuss some of the properties of the adiabatic states and the adiabatic eigenvalues and present numerical examples, interpreted in terms of adiabatic states, that demonstrate complete population transfer. We will point out some peculiar features of the transfer process, readily overlooked, that are related to the properties of the RWA Hamiltonian.

D. Concerns: Intermediate-state population

In a typical application of basic three-state STIRAP the initial and the final states are long lived, but the in-

termediate state is shorter lived and, if populated, will lose population by spontaneous emission into states other than the three of interest. The three-state STIRAP process avoids such losses by moving population directly between the initial and the final states without placing any population into the intermediate state. The procedure is accomplished by maintaining population in an adiabatic dressed state that has no component of the intermediate atomic state.

In more general cases, involving magnetic sublevels, it may not always be possible to create completely "dark" dressed states (i.e., dressed states that have no component of any of the intermediate sublevels). In such cases adiabatic passage will place some population into the intermediate sublevels. The presence of intermediate-state populations need not hinder complete population transfer between selected sublevels, if decay from intermediate levels is negligible. However, the presence of numerous adiabatic energies raises new concerns. We discuss the need to show that, for adiabatic passage to cause population transfer, there should be an adiabatic connection between a single initial sublevel and a desired single final sublevel (one for which two-photon resonance applies). When such a connection occurs, a counterintuitive pulse sequence conducted adiabatically will induce complete population transfer.

Transient transfer of population into intermediate sublevels is affected by single-photon detunings. We find instances in which it is desirable to operate with some single-photon detuning, unlike the pure three-state STIRAP where single-photon resonance is desirable.

E. STIRAP verification

To demonstrate STIRAP one must demonstrate (essentially) complete population transfer to a single final state. This must take place as coherent excitation. When sublevels are present, it is neccessary to measure the distribution of population among the final sublevels.

In the absence of deliberate control, the terrestrial magnetic field will scramble the sublevels during time intervals longer than the relevant Larmor precession period. For best results the populations should not move among the sublevels during the time between the end of the STIRAP process and the moment of population probing. To ensure this state stability one can impose a static magnetic field which will produce Zeeman splitting of the various sublevels and will maintain sublevel distinctness. Thus verification of the population transfer requires some control of the static magnetic field and we need to know how this splitting, if present during the course of the STIRAP process, will affect population transfer.

II. MULTISTATE RWA HAMILTONIAN AND LINKAGES

A. Nine-state RWA Hamiltonian

Throughout the remainder of this paper we consider only a specific example, appropriate to the excitation of metastable neon, in which an initial level of angular momentum $J = 0$ proceeds to a final level having $J = 2$, through an intermediate level of $J = 1$. This system, though less general than other choices, illustrates the major properties of coherent excitation with sublevels.

The first step toward analyzing coherent excitation is to establish the linkage pattern of the RWA Hamiltonian. Such diagrams show, in simple cases, the excitation route from initial to final state. In more general cases they merely show the several sublevels that may participate in the population dynamics. For electric (or magnetic) dipole radiation, considered here, each magnetic sublevel has a link with no more than three sublevels of the adjacent levels in the chain. Thus the most general linkage pattern is that of Fig. 1. This figure defines the numbering convention that we hereafter follow. For clarity this figure shows the linkage pattern as it would be appropriate for a ladder system, wherein successive levels increase in energy, rather than for a Λ (or Raman) sequence, in which the first and the last levels have lower energy than the middle level. The details of this matrix depend on the angular momentum quantum numbers J and M of the various sublevels and upon the polarization directions of the two radiation fields; it may be evaluated by applying standard procedures from the quantum theory of angular momentum [50,51]. As we note below, for several special choices of polarizations the general pattern reduces to conventional STIRAP process involving only three linked sublevels.

The introduction of a rotating-wave picture for probability amplitudes follows the same procedure in an angular momentum basis as it does for nondegenerate states (see [11], Chap. 20). For simplicity we choose the quantization axis of the angular momentum states to coincide with the direction of the magnetic field. With this choice the evaluation of the magnetic interaction is trivial: the magnetic interaction Hamiltonian is a diagonal matrix whose elements are the usual Zeeman shifts given by the product of the magnetic quantum number M, the Landé g factor, the Bohr magneton, and the magnetic field strength. The diagonal elements of the RWA Hamil-

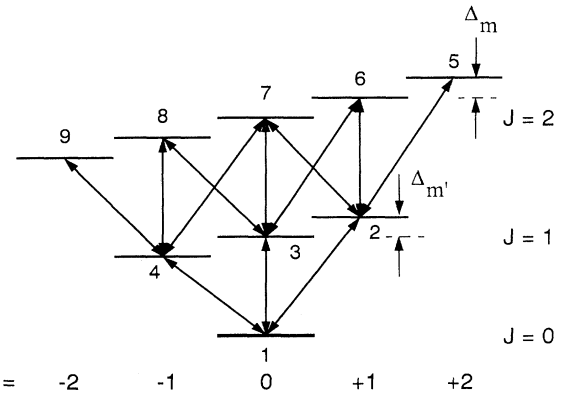

FIG. 1. Numbering convention and potential linkage patterns for the nine sublevels of the transitions $J = 0 \Leftrightarrow 1 \Leftrightarrow 2$, exhibited as a ladder system. The Zeeman splittings of the intermediate and the final levels are $\Delta_{m'}$ and Δ_m, respectively.

tonian become detunings between laser carrier frequencies and Zeeman-shifted Bohr frequencies.

For the $J = 0 \Leftrightarrow 1 \Leftrightarrow 2$ sequence that we are considering the upper triangular portion of the RWA Hamiltonian (times $2/\hbar$) for a Λ configuration has the form

$$\begin{bmatrix} 0 & \Omega_P K_{12} & \Omega_P K_{13} & \Omega_P K_{14} & 0 & 0 & 0 & 0 & 0 \\ \cdots & 2\Delta_P + 2\Delta_{m'} & 0 & 0 & \Omega_S K_{25} & \Omega_S K_{26} & \Omega_S K_{27} & 0 & \\ \cdots & \cdots & 2\Delta_P & 0 & 0 & \Omega_S K_{36} & \Omega_S K_{37} & \Omega_S K_{38} & 0 \\ \cdots & \cdots & \cdots & 2\Delta_P - 2\Delta_{m'} & 0 & 0 & \Omega_S K_{47} & \Omega_S K_{48} & \Omega_S K_{49} \\ \cdots & \cdots & \cdots & \cdots & 2\Delta_d + 4\Delta_m & 0 & 0 & 0 & 0 \\ \cdots & \cdots & \cdots & \cdots & \cdots & 2\Delta_d + 2\Delta_m & 0 & 0 & 0 \\ \cdots & \cdots & \cdots & \cdots & \cdots & \cdots & 2\Delta_d & 0 & 0 \\ \cdots & \cdots & \cdots & \cdots & \cdots & \cdots & \cdots & 2\Delta_d - 2\Delta_m & 0 \\ \cdots & \cdots & \cdots & \cdots & \cdots & \cdots & \cdots & \cdots & 2\Delta_d - 4\Delta_m \end{bmatrix}.$$

The factors Ω_P and Ω_S are sublevel-averaged Rabi frequencies that, being proportional to electric field amplitudes, contain all of the time dependence. The time-independent dimensionless coupling coefficients K_{ij}, discussed in the following sections, contain the dependence on the polarization directions (see the Appendix for a discussion of the derivation of these factors). The frequencies $\Delta_{m'}$ and Δ_m are Zeeman shifts for levels 2–4 and 5–9 respectively. As diagrammed in Fig. 2, the frequency Δ_P is the detuning of the pump frequency ω_P from the unshifted pump transition and Δ_d is the difference between pump and Stokes frequency shifts (i.e., the Raman frequency or detuning from two-photon resonance).

B. Specialization to linear polarization

The procedure for calculating the Rabi frequency for arbitrary (elliptically) polarized light is presented in the Appendix. Formula (A2) presents the basic dependence upon magnetic quantum numbers. To simplify the discussion, we consider linear polarizations for both fields. When the polarization axis is used as the quantization axis, then the electric field lies along one unit vector and only the $q = 0$ component occurs in the sum. For more generality we let the quantization axis be arbitrary.

To connect the electric-field vector in this reference frame with the vector in another frame (e.g., that of the static magnetic field), we require a rotation matrix of order 1:

$$\mathbf{e}(\alpha,\beta,\gamma)_q = \mathcal{D}^{(1)}_{q0}(\alpha,\beta,\gamma)\mathbf{e}_0. \tag{2.1}$$

We therefore obtain the formula

$$\Omega(J_1M_1;J_2M_2) = \sum_q \bar{\Omega}\mathcal{D}^{(1)}_{q0}(\alpha,\beta,\gamma)(-1)^{J_1-M_1}\begin{pmatrix} J_1 & 1 & J_2 \\ -M_1 & q & M_2 \end{pmatrix}, \tag{2.2}$$

where the reduced matrix element and the pulse envelope have been incorporated into the sublevel-averaged Rabi frequency $\bar{\Omega}$

$$\bar{\Omega} = -\frac{\mathcal{E}^*_P}{\hbar}(J_1||d||J_2). \tag{2.3}$$

Note that only a single term occurs in the sum $q = M_1 - M_2$. The dependence upon angles enters as

$$\sqrt{2}\mathcal{D}^{(1)}_{q0}(\alpha,\beta,\gamma) = \begin{cases} \sin\beta\exp(i\alpha) & \text{for } q = +1 \\ \sqrt{2}\cos\beta & \text{for } q = 0 \\ -\sin\beta\exp(-i\alpha) & \text{for } q = -1. \end{cases} \tag{2.4}$$

For the present discussion we consider copropagating or counterpropagating linearly polarized pump and Stokes lasers with electric-field vectors lying in a common plane with the magnetic-field direction, so that only a single angle β need to be specified for each laser field. Figure 3 shows the assumed geometry. Under these simplifications the coupling coefficients are

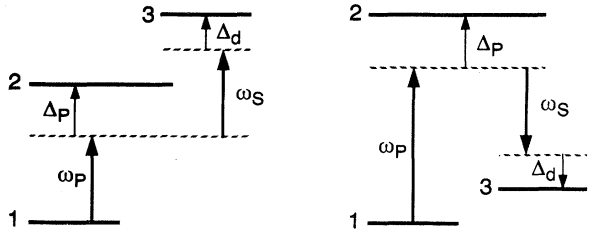

FIG. 2. Definitions of pump frequency ω_P, pump detuning Δ_P, Stokes frequency ω_S, and two-photon detuning Δ_d for the ladder configuration (left) and Λ configuration (right).

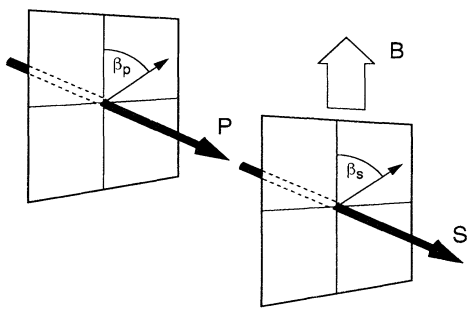

FIG. 3. Definition of pump polarization angle β_P and Stokes polarization angle β_S with respect to the B field and propagation directions, for collinear laser beams.

$$K_{12} = \sqrt{\frac{1}{6}}\sin\beta_P,\ K_{13} = -\sqrt{\frac{1}{3}}\cos\beta_P,\ K_{14} = -K_{12} \tag{2.5a}$$

and

$$K_{25} = \sqrt{\frac{1}{10}}\sin\beta_S,\ K_{26} = \sqrt{\frac{1}{10}}\cos\beta_S,\ K_{27} = -K_{47}, \tag{2.5b}$$

$$K_{36} = \sqrt{\frac{1}{20}}\sin\beta_S,\ K_{37} = \sqrt{\frac{2}{15}}\cos\beta_S,\ K_{38} = -K_{36}, \tag{2.5c}$$

$$K_{47} = \sqrt{\frac{1}{60}}\sin\beta_S,\ K_{48} = \sqrt{\frac{1}{10}}\cos\beta_S,\ K_{49} = -K_{25}, \tag{2.5d}$$

where the subscripts P and S refer to pump and Stokes polarization directions. When β_P and β_S are not 0° or 90°, all the matrix elements are nonzero and then coupling exists among all sublevels. Note that the choice of pump polarization angle

$$\tan\beta_P = \sqrt{2} \qquad \text{or} \qquad \beta_P = 54.7° \tag{2.6}$$

equalizes the three components of the pump dipole transition moments. This is the so-called magic angle, where there occurs a zero of the second Legendre polynomial. No single angle will give equality among the transition moments for the Stokes transition.

C. Simple linkage patterns

Inspection of the RWA Hamiltonian matrix reveals several special choices of polarizations for which the ground state has links only to a three-state chain, as in conventional STIRAP. Figure 4 shows some of these cases.

The simplest case occurs when pump and Stokes fields are each linearly polarized, and these polarizations are in the direction of the static magnetic field. Then we have the conventional STIRAP process, involving only transitions between states having $M = 0$. Figure 4(a) shows the linkage pattern in this case, simplified by presenting it as would be appropriate for a ladder rather than for a Λ sequence. Light lines indicate linkages that do not participate in the coherent dynamics evolving from state 1. These linkages do have an important effect when spontaneous emission (optical pumping) alters populations significantly. As can be seen, only states 1, 3, and 7 participate in the coherent excitation dynamics. Because these sublevels have null Zeeman shift, one- and two-photon resonance occurs when the carrier frequencies are resonant with the unshifted transitions.

Other simple three-state cases occur when the pump and Stokes fields are circularly polarized and they propagate collinearly along the direction of the static magnetic field. When the polarizations have the same sense (for a ladder configuration), one can transfer population entirely to $|M| = 2$ [see Fig. 4(b)], whereas when the polarizations have the opposite sense, population transfer to $M = 0$ takes place. Again, heavy lines indicate the transitions that participate in the coherent excitation and light lines show linkages between unpopulated states.

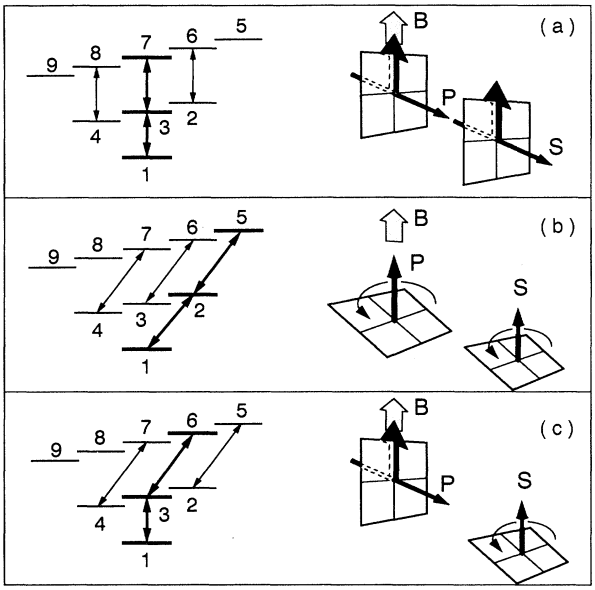

FIG. 4. Examples of three-state linkage patterns that can be obtained by suitable choice of polarizations: (a) both fields linearly polarized along a common axis, (b) both fields circularly polarized with the same sense along a common axis, and (c) combination of linear and circular polarization, with beams not collinear.

By careful orientation of pulse propagation directions to be at right angles, it is possible to combine a linearly polarized pulse with a circularly polarized pulse to produce the linkage patterns shown in Fig. 4(c). Note that this is not a case described by the explicit formulas above, involving collinear beams. In all of these cases the presence of angular momentum introduces no additional effects beyond the basic three-state STIRAP considerations.

D. General linkages

When the pump and the Stokes polarizations are not collinear, then the Hamiltonian may become more complicated and linkages may connect more than three sublevels. In such cases interference may occur between alternative paths between connected states and it is not always possible to guess the dynamic behavior of the system from inspection of a linkage diagram. Nevertheless, the linkages do show possible excitation routes and can be useful guides.

Figure 5 shows linkages that occur when the fields are linearly polarized but in orthogonal directions. For

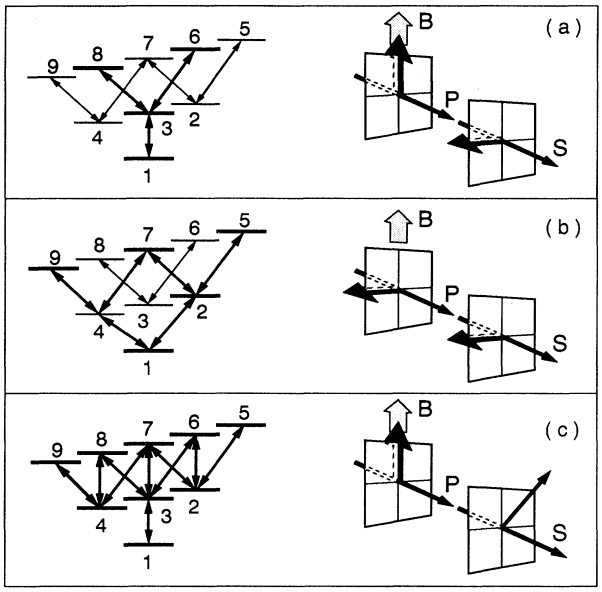

FIG. 5. Examples of multiple-state linkage patterns that can be obtained by suitable choice of polarizations: (a) pump field linearly polarized along the B field, Stokes field linearly polarized at right angles to this; (b) pump and Stokes fields polarized linearly at right angles to the B field; and (c) Stokes field linearly polarized at 45° to pump.

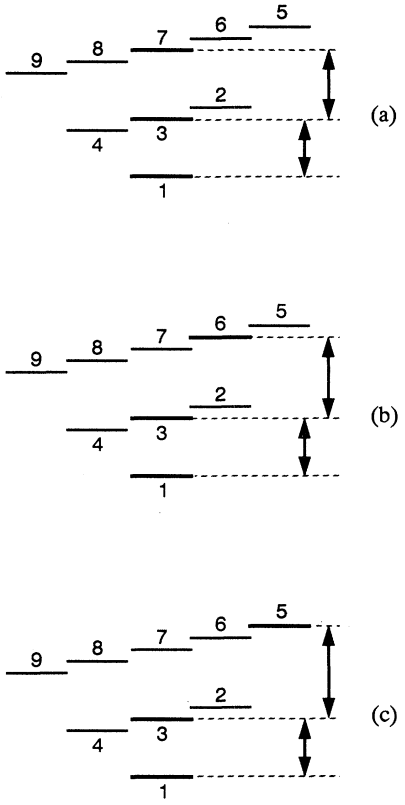

FIG. 6. Two-photon resonance conditions for (a) state 7, (b) state 6, and (c) state 5, in a ladder configuration.

$\beta_P = 0$ this gives rise to the linkage of Fig. 5(a) involving a single intermediate sublevel and two final sublevels. In the absence of spontaneous emission, only two of the final states are coupled to the ground state. These linkages are shown as heavy lines; light lines indicate the transitions among unpopulated states. When Zeeman splitting is present (and is larger than the two-photon linewidth established by the peak Rabi frequencies) then only one of these final states will satisfy the two-photon resonance condition. An example involving three final sublevels, realized for $\beta_P = \beta_S = 90°$, is shown in Fig. 5(b). When the pump polarization lies along the magnetic field but the Stokes polarization does not, we obtain the linkages of Fig. 5(c). All sublevels are interconnected in this case.

The more general pattern of Fig. 1 occurs for arbitrary elliptic polarization or for linear polarization with neither β_S or β_P taking the values 0° or 90°. A very simple arrangement in which this linkage obtains occurs when the pump and the Stokes beams are collinear, propagating perpendicular to the B field, and with linear polarization at 45° with respect to each other.

E. Resonance conditions

The linkage pattern of Fig. 5(c) suggests that population could reach all of the final magnetic sublevels. (That is, the dressed state introduced by the Stokes field contains components of all of the magnetic sublevels.) However, the presence of population in any state will depend upon the presence of resonant tuning in the various linkages; common experience suggests that resonant transitions will produce larger population transfers. When the sublevels exhibit Zeeman splitting, then the various transitions cannot all be resonant simultaneously. As a rule, we require that the pump and the Stokes frequencies combine to produce a two-photon resonance with the desired final state. One of the intermediate states may also be resonant with the pump transition, but this is not always desirable. Figure 6 shows the one- and the two-photon resonance conditions for a ladder configuration.

III. LOSSLESS POPULATION TRANSFER DYNAMICS

A. Dynamical eigenvalue structure

The dressed states of the lossless RWA Hamiltonian, which provide the adiabatic states that are employed in the STIRAP processes, can be assigned labels that identify the placement of the associated eigenvalue in an ordered list of eigenvalues. For example, the adiabatic state that has the second largest eigenvalue will at all times be uniquely defined, barring degeneracy. This property of the adiabatic states makes it possible to deduce the adiabatic behavior of a pulsed excitation sequence by examining a plot of RWA eigenvalues versus time. Both

initially and finally the eigenvalues are the diagonal elements of the RWA Hamiltonian (the detunings) and so at these times the curves have a unique connection (barring degeneracy) with particular atomic states. By following a curve that avoids all crossings we deduce the connection between initial and final atomic states.

It is this connectivity property of dressed eigenvalues that offers the possibility for producing, by adiabatic passage, complete population transfer between an initial atomic state and another atomic state for which the laser carrier frequencies maintain resonance. What cannot be determined from the eigenvalue curves are the details of the transition and whether a particular pulse arrangement does in fact maintain adiabatic conditions.

B. Examples of population transfer without loss

In the following examples we illustrate this adiabatic population transfer in a three-level atom having $J = 0, 1,$ and 2, and with Zeeman splitting $\Delta_{m'} = \Delta_m$ as is appropriate for levels of ^3P (as occurs with metastable neon). There exists a nondenumerable infinity of possible choices for polarization angles and detunings for which adiabatic population transfer can be accomplished in the absence of spontaneous emission.

Population transfer to $J = 2, M = 0$ could readily be accomplished by choosing pump and Stokes polarizations to both be linearly polarized along the magnetic-field direction; as noted above the linkage pattern then becomes that of the conventional three-state STIRAP. Similarly, population transfer to $|M| = J$ could be accomplished by using circularly polarized light that again reduces the linkage pattern to three states. However, such arrangements of polarizations do not permit other choices of final sublevels. Therefore we here consider an arrangement that has potential linkages to all sublevels: we take the Stokes field to be linearly polarized at 45° to the collinear pump and magnetic-field direction ($\beta_P = 0°, \beta_S = 45°$). Under these conditions all of the magnetic sublevels of the final ($J = 2$) level have some linkage with the ground state. We shall show that, with this arrangement, it is possible (if decay is negligible) to place all population into a single sublevel by setting the combined pump and Stokes frequencies to match the two-photon resonance conditions with a selected sublevel.

There are several options for choosing the single-photon detunings. For the examples presented here we have taken the pump to be at a fixed frequency, not resonant with any of the excited states, and we vary the Stokes detuning to establish two-photon resonance with the desired final state. Specifically, we choose

$$\Delta_{m'} = \Delta_m = 0.3 \text{ rad/ns}, \qquad \Delta_P = 0.6 \text{ rad/ns}. \quad (3.1a)$$

As pulse shapes we have taken the electric-field amplitude to be proportional to one cycle of a squared sinusoid

$$\Omega_S(t) = \Omega_S^{\max} \sin^2(\pi t/T),$$
$$\Omega_P(t) = \Omega_P^{\max} \sin^2(\pi t/T - \pi t_P/T). \quad (3.1b)$$

This functional form, unlike the often used Gaussian pulse, goes exactly to zero at finite times, taken here to be $t = 0$ and $t = T$ for the Stokes pulse. For the following figures we used the parameters

$$\Omega_{P,S}^{\max} = 3 \text{ rad/ns}, \qquad T = 6000 \text{ ns}, \qquad t_P = 2000 \text{ ns}. \quad (3.1c)$$

The following set of figures shows examples of complete population transfer to a final magnetic sublevel that has been selected by adjusting the Stokes frequency, holding fixed the two polarizations and the pump frequency. The top frame shows the pump and the Stokes envelopes. The middle frame shows the adiabatic eigenvalues obtained by diagonalizing the RWA Hamiltonian at each instant of time. The bottom frame shows the population histories obtained from numerical solution to the time-dependent Schrödinger equation.

C. Examples: Population transfer to $M = 0, +1,$ and $+2$

Figure 7 shows the behavior when we enforce two-photon resonance with the $M = 0$ sublevel of the fi-

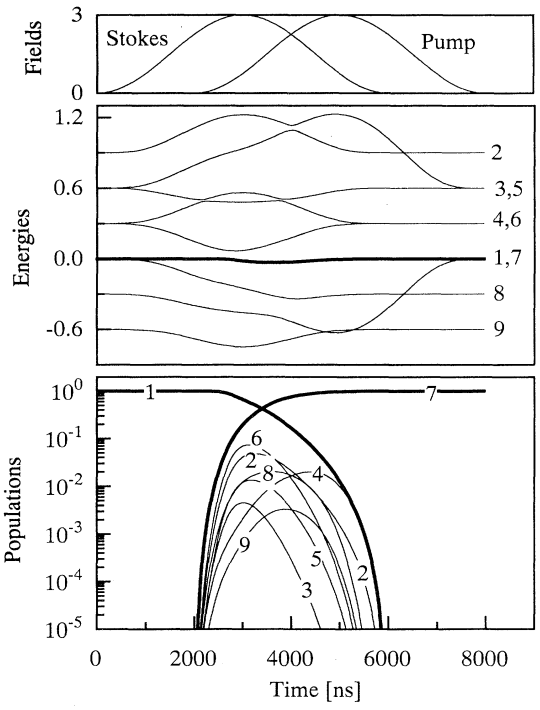

FIG. 7. Example of time evolution for lossless nine-state system. The top frame shows envelopes of pump and Stokes pulses; the middle frame shows adiabatic eigenvalues (the heavy line is the STIRAP state); the bottom frame shows population histories. Heavy lines are states between which STIRAP occurs. The pump is detuned from the single-photon resonance ($\Delta_P = \Delta_S = 0.6$ rad/ns), Zeeman splittings $\Delta_{m'} = \Delta_m = 0.3$ rad/ns, and polarization angles are $\beta_P = 0°$ and $\beta_S = 45°$. For this example two-photon resonance occurs with $M = 0$ (state 7).

nal level (atomic state 7). From the bottom frame we see that complete population transfer occurs into the desired sublevel, just as it would for conventional three-state STIRAP, despite the linkages to other states. It should be noticed that, although population transfer is eventually complete, during the process there is transient population (about 10%) in two intermediate sublevels (atomic states 2 and 4). This population can undergo spontaneous emission and therefore its presence may limit population transfer and selectivity.

We can track the course of adiabatic population transfer on the energy diagram in the center frame. The initial and the final spread of dressed eigenvalues represents the spread of Zeeman shifts. In the absence of pulsed radiation interaction our choice of Zeeman splittings, taken with the energy conventions of the RWA, leads to degeneracies of atomic states 1 and 7, states 3 and 5, and states 4 and 6. The pulsed radiation field removes this degeneracy. The eigenvalue of interest here is the fourth one; it remains nearly zero at all times and connects the initial atomic state 1 with the final atomic state 7. Transient population occurs in each of the intermediate sublevels. In this case each of the sublevels of the intermediate level (states 2–4) obtains transient population; there is no dark state.

This same arrangement of polarizations, with attendant sublevel linkages, can be used to place population into any of the other final sublevels. Figure 8 shows population transfer into the final $M = +1$ sublevel (atomic state 8) that occurs when the detunings are chosen to make only that sublevel resonant. In this case it is the third eigenvalue that is associated with the STIRAP state

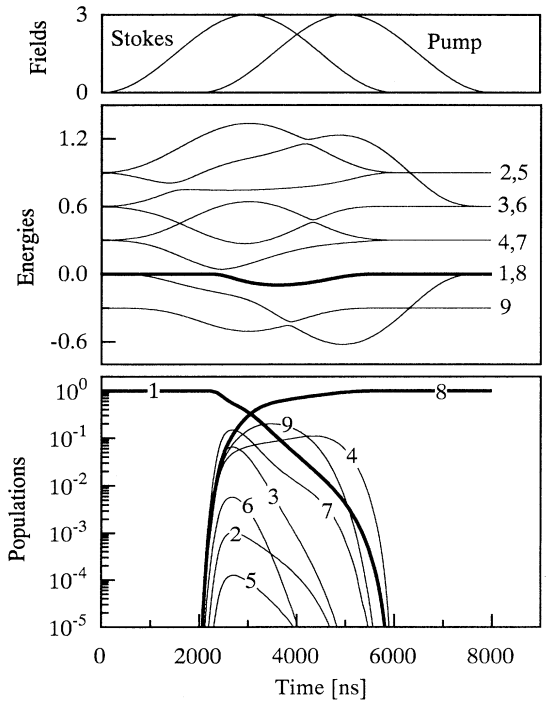

FIG. 8. Same as in Fig. 7 but with two-photon resonance with $M = 1$ (state 8).

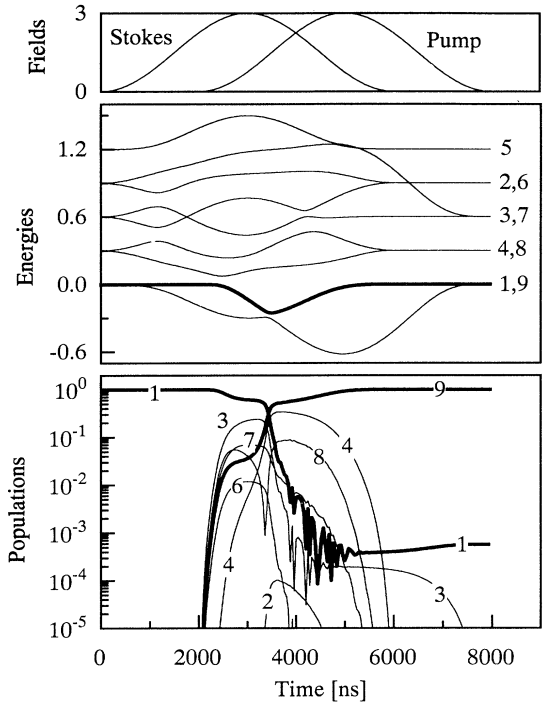

FIG. 9. Same as in Fig. 7 but with two-photon resonance with $M = 2$ (state 9).

and it deviates noticeably from zero during the pulse sequence. As with the previous example, there is no dark state.

Figure 9 shows the population transfer that occurs into the $M = +2$ sublevel (atomic state 9) when this sublevel obeys the two-photon resonance condition and the other parameters are as chosen for the previous figures. The eigenvalue of interest here is the second one. From the eigenvalue plots it can be seen that there is a close approach of neighboring eigenvalues at two intermediate times. This hints that there may be difficulty in maintaining adiabatic conditions. The particular choice of pulses used here produce successful population transfer, but an inspection of data from a large set shows that small changes of operating conditions could cause transfer to fail.

An examination of the linkage pattern suggests that this might be regarded as a four-photon resonance (one pump and three Stokes interactions are associated with the simplest links between initial and final atomic states). This interpretation is consistent with the observation that higher Rabi frequencies are required to produce population transfer with this choice of polarizations than is the case for polarizations that provide direct linkages between states 1 and 9.

D. Asymmetries in population transfer to $M = +2$ and -2

Resonance conditions must be considered when one examines the linkage patterns. Figure 10 shows examples.

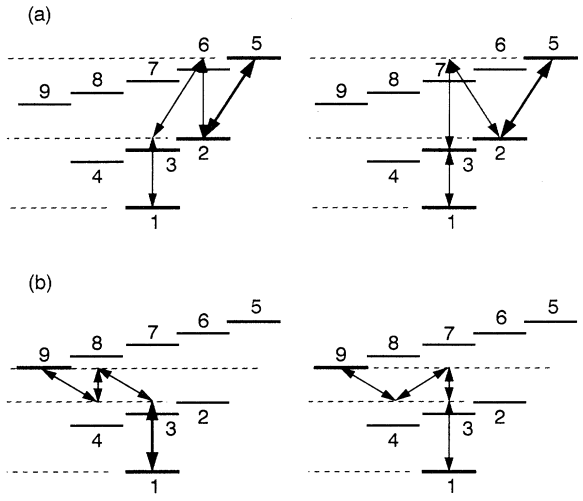

FIG. 10. (a) Four-photon sequence 1-3-6-2-5 between states 1 and 5. (b) Four-photon sequence 1-3-7-2-5 between states 1 and 5. (c) Four-photon sequence 1-3-8-4-9 between states 1 and 9. (d) Four-photon sequence 1-3-7-4-9 between states 1 and 9.

The top two frames show connections to $M = +2$ (state 5) through the linkages

$$1 \Leftrightarrow 3 \Leftrightarrow 6 \Leftrightarrow 2 \Leftrightarrow 5 \quad \text{[sequence (a)]},$$

$$1 \Leftrightarrow 3 \Leftrightarrow 7 \Leftrightarrow 2 \Leftrightarrow 5 \quad \text{[sequence (b)]}.$$

As shown at the bottom, two frames connections to $M = -2$ (state 9) occur through the linkages

$$1 \Leftrightarrow 3 \Leftrightarrow 8 \Leftrightarrow 4 \Leftrightarrow 9 \quad \text{[sequence (c)]},$$

$$1 \Leftrightarrow 3 \Leftrightarrow 7 \Leftrightarrow 4 \Leftrightarrow 9 \quad \text{[sequence (d)]}.$$

These are the most direct routes between these initial and final sublevels, although there is an infinite number of other routes involving multiple connections and multiple loops. When the pump is resonant with state 3, then both of these sequences (to $M = +2$ and $M = -2$) have the same absolute values of intermediate detunings and hence they will produce symmetric distributions into $M = +2$ and $M = -2$. However, when the pump is not resonant, then the two sequences will not have the same absolute values for these detunings and one expects differences in the populations reaching the final states via two-photon resonance and STIRAP. Figure 10 offers some insight into the expected behavior. All of these sequences satisfy a two-photon resonance condition that could arise when the pump is tuned to the blue side of resonance. The first two frames show two of the possible connections between states 1 and 5 when the two-photon resonance is to state 5. There are two intermediate non-resonant detunings, but the final linkage is resonant. Note that the matrix element products $K_{36}K_{26}$ and $K_{37}K_{27}$ that occur in the two sequences above each involve the product $\sin\beta_S\cos\beta_S$, so that the ratio of these products is unaffected by change in Stokes polarization β_S.

In the second sequence, with two-photon resonance established to state 9, there are no intermediate resonances. Although each of these sequences requires a minimum of four photons, we would expect that the sequence to state 5 would have a stronger connection between initial and final states. Numerical modeling shows that higher Rabi frequencies are needed for complete transfer to level 9 as compared to level 5, for the tuning of the laser frequencies shown in Fig. 10. Numerical modeling (see below) also shows that the occurrence of pump-laser resonance tunings (with level 2 as examplified in Fig. 10) can have detrimental effects upon population transfer into final sublevels.

E. Population transfer to the intermediate states

In conventional three-state STIRAP the intermediate state does not participate in the adiabatic dynamics; the process is possible with or without resonance of the single-photon detunings. When the system has more complicated linkage patterns, then in general the intermediate states participate in an essential way and the behavior can depend qualitatively upon the status of single-photon detunings. An interesting possibility occurs, in the example of $\beta_P = 0°$ and $\beta_S = 45°$ polarizations treated above, when the pump field is resonant with the $M = +1$ sublevel of the intermediate level and there is no exact two-photon resonance. Under these conditions complete population transfer occurs to the only

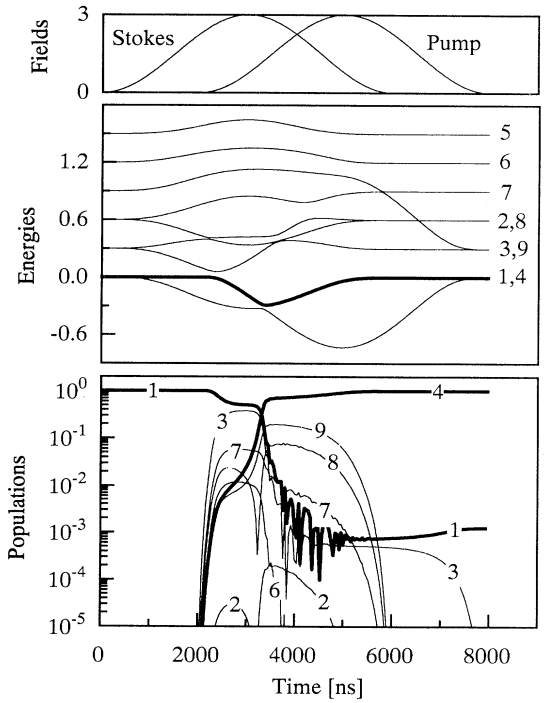

FIG. 11. Same as in Fig. 7 but with the pump field resonant with $M = 1$ (state 4). Population is transferred to state 4.

resonant final state, the $J = 1, M = 1$ intermediate state. This particular state is not directly connected to the ground state (the linearly polarized pump only connects the $J = 1$, $M = 0$ state to this); the connection can be regarded as a three-photon resonance (one pump and two Stokes interactions; see Fig. 10). Figure 11 illustrates this case.

For application to STIRAP-type population transfer, it is not desirable to place population into intermediate states, either temporarily or finally, because these states have connections, via spontaneous emission, to atomic states that are immune to excitation by the pulsed radiation. We can recognize, from the present example, that any pump resonances with intermediate Zeeman-shifted sublevels can be detrimental to the STIRAP process, unless conditions are identified that make all three intermediate basis states dark. This possibility will be discussed in a companion paper [49].

F. Degeneracies and connectivity

To maintain the state vector as a single dressed state (e.g., the STIRAP state) there must be no possibility of mixing this state with another dressed state. This condition requires that the null eigenvalue remain well separated from other eigenvalues. If this is not the case, then we may expect that population transfer will not be complete and that population histories may exhibit oscillations. Alternatively, successful population transfer may occur by following diabatic evolution through curve crossings. Potential problems can be revealed by examining plots of eigenvalues. Figure 12 presents qualitative examples of two sets of adiabatic eigenvalue curves, for the smallest magnitude eigenvalues. In the upper case there is an adiabatic connection between desired atomic states relating to zero eigenvalues when one of the Rabi frequencies is zero and adiabatic passage will transfer population. In the lower frame there is no such adiabatic connection and the maintenance of adiabaticity will not produce population transfer. These problems and a strategy of how to identify them are discussed in the following paper [49].

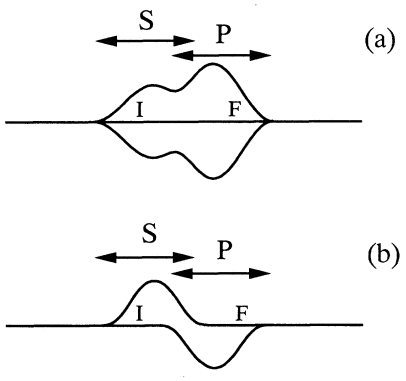

FIG. 12. Examples of adiabatic connections, with changing time as the horizontal axis, between adiabatic states at early times (left) and adiabatic states at late times (right). Arrows show regions of pump and Stokes pulses. (a) Triple degeneracy of null eigenvalue initially and finally, with an adiabatic connection between desired initial (I) and final (F) atomic states. (b) Double degeneracy initially and finally, with no adiabatic path between desired initial (I) and final (F) atomic states.

IV. POPULATION TRANSFER WITH LOSS

A. Effects of spontaneous emission

The demonstration of population transfer by means of the Schrödinger equation, while desirable for its simplicity and insights, does not adequately describe the physical situations that occur in practice. It is essential to consider effects of spontaneous emission, which transfers population between sublevels, diminishes coherences, and introduces population loss from the manifold of states that are treated. We incorporate all of these effects with the aid of the density matrix. We have found that parameter choices that appear satisfactory for completely coherent excitation may be poor choices when spontaneous emission is included. Nevertheless, our calculations suggest that, for realistic values of pulse duration and peak intensity, it should be possible to achieve population transfer close to the adiabatic ideal.

B. Choice of polarizations

Simple considerations based on linkage patterns suggest that certain choices of polarizations and detunings are particularly suited to population transfer into certain final states. Other choices are expected to be detrimental. A satisfactory choice is to take the pump polarization to be at the angle that equalizes the three components of the pump dipole transition moments. [This occurs at the so-called magic angle, for which Eq. (2.6) holds.] In Ref. [49] we show that when two-photon resonance exists to state 7 we can force a null-eigenvalue state by the requirement

$$\tan\beta_S = 2\tan\beta_P. \tag{4.1}$$

Here we quantify those simple predictions by showing the dependence of the population transfer efficiency on the two polarization angles of linearly polarized collinear pulses. Figure 13 shows the effect of polarization choices on adiabatic population transfer into states 7–9, for the parameter choices specified in Table I. States 5 and 6, not shown here, have behavior like that of states 9 and 8. For these calculations we fixed the frequencies to force a two-photon resonance between the starting state 1 and the final state of interest, but we avoided single-photon resonances.

The figures show, as expected from earlier discussion, that the polarization choice $\beta_P = 0$ and $\beta_S = 0$, making polarizations collinear with the quantization axis, produces nearly complete population transfer into state 7 (for which $M = 0$). The polarization choice $\beta_P = 90°$

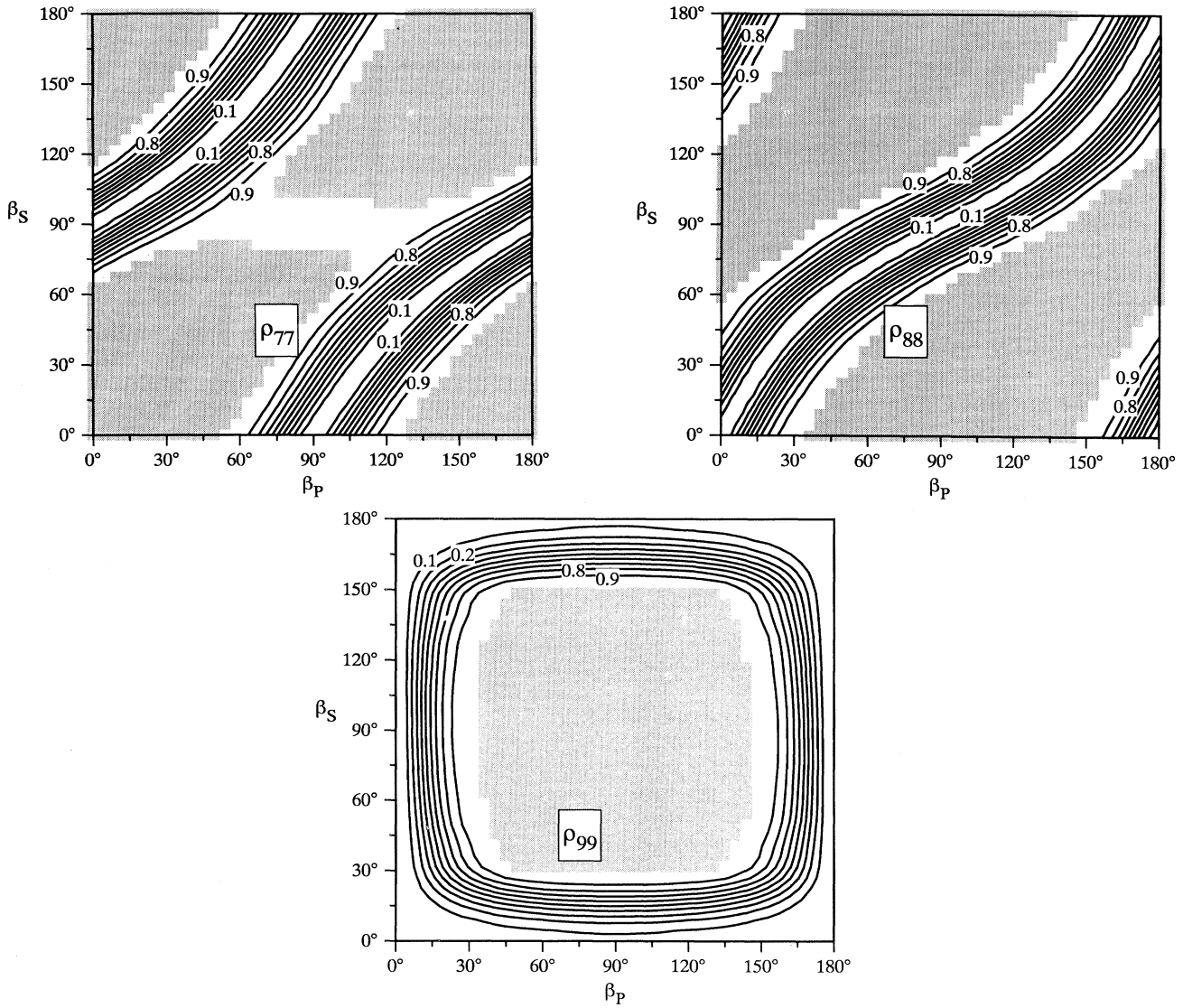

FIG. 13. Contour plots of populations reaching selected final states, as a function of pump polarization angle and Stokes polarization angle. The pump field is not resonant ($\Delta_P = 6.28$ rad/ns). Selected final states are $M = 0$ (state 7, upper frame), $M = +1$ (state 8, center frame), and $M = +2$ (state 9, lower frame). Regions where transfer efficiency exceeds 95% are gray. The parameters are given in Table I. In each case the Stokes laser frequency is chosen to establish the appropriate two-photon resonance condition.

TABLE I. Parameters used for calculating Fig. 13. $\Omega_P^{\max}$ and $\Omega_S^{\max}$ are the Rabi frequencies for the pump laser (P) and Stokes laser (S). Δ_P and Δ_S are detunings from resonance with level 3 for the pump laser (P) and the Stokes laser (S). The Zeeman splitting of the intermediate levels (2–4) is $\Delta_{m'}$ and the splitting of the final levels (5–9) is Δ_m. The A_{ik} with $i = b$ and $k \in \{a, b, c\}$ are the Einstein coefficients; a stands for the intial state (1), b for the intermediate states (2–4), c for the final states (5–9), and d for the sum of all additional states that will not be part of the coherent STIRAP process but could receive population through spontaneous emission.

$\Omega_P^{\max} = 6.28$ rad/ns	$\Omega_S^{\max} = 6.28$ rad/ns	$A_{ba} = 0.0151$ ns^{-1}
$\Delta_P = 6.28$ rad/ns	$\Delta_S = 6.28$ rad/ns	$A_{bc} = 0.0110$ ns^{-1}
$\Delta_{m'} = 3.14$ rad/ns	$\Delta_m = 3.14$ rad/ns	$A_{bd} = 0.0287$ ns^{-1}

and $\beta_S = 0°$, or the choice $\beta_S = 90°$ and $\beta_P = 0°$, for which one polarization is at right angles to the quantization axis, produces nearly complete population transfer into states 6 and 8 (for which $M = +1$ and -1).

On such plots the regions of high transfer efficiency will further increase as the peak Rabi frequencies and Zeeman splittings are increased. When the peak Rabi frequencies become sufficiently large, there occur polarization choices that permit high efficiency transfer into *any* desired final state, just by choosing the right frequency for two-photon resonance. (Conversely, if the Rabi frequencies are too small, there will exist no such region of high efficience common to all final states.) One example of such a choice, in which all final sublevels can be reached, is

$$\beta_P = 75°, \quad \beta_S = 45°. \tag{4.2}$$

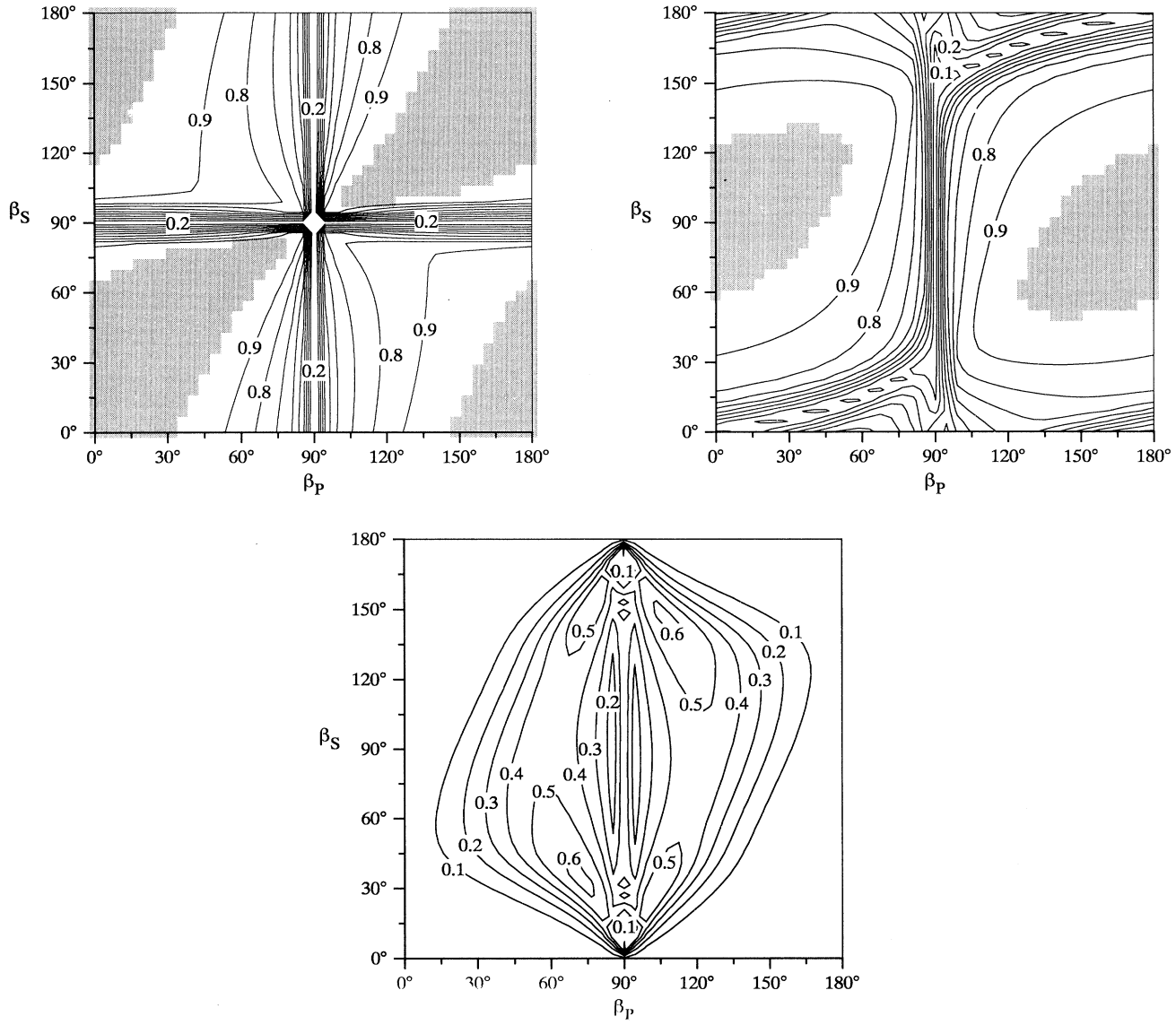

FIG. 14. Same as in Fig. 13 but the pump field is resonant with state 3 ($M = 0$).

This choice, marked by a box surrounding the inset ρ_{ii} ($i = 7$–9) in Fig. 13, is appropriate to the particular pump detuning chosen for these calculations.

The sensitivity to polarization angles, shown here, is not great when there is no single-photon resonance. However, when the pump frequency matches a one-photon resonance, then calculations show that population transfer will be poor into states 5 and 9 (less than 50%) for any choice of polarization. Examples of these cases are shown in Fig. 14. In these cases there is no single choice of polarization angles that will produce transfer efficiency above 90% to all of the final sublevels.

C. Effect of detuning

Because it is more convenient to vary the frequency of one laser rather than to vary the polarizations, it is desirable to be able to control population transfer by frequency selection alone. Figure 13 shows that, in principle, this objective should be attainable. For the following computations we chose polarization directions such that all possible final states have links with the ground state, specifically the angles $\beta_P = 75°$ and $\beta_S = 45°$.

To interpret these results it is useful to view the locus of points where one- and two-photon resonances occur, as presented in Fig. 15. In this figure and the plots of Fig. 16 the locus of two-photon resonance values follows a straight line diagonally across the frame (the intercept of this line differs for different sublevels, according to their different Zeeman shifts). The locus of pump resonance values is a vertical line. We expect that adiabatic population transfer will occur along the diagonals of this plane. We expect that single-photon resonances, along the loci shown, will affect the transfer.

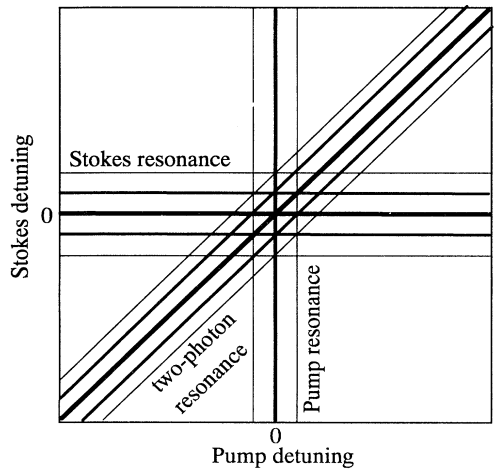

FIG. 15. Locus of points that produce resonance detuning. Vertical lines are single-photon resonances for the pump field, horizontal lines are single-photon resonances for the Stokes field, and the lines at 45° are two-photon resonances.

Figure 16 shows examples of final state population, transferred adiabatically by counterintuitive pulse sequence, as a function of pump detuning and Stokes detuning. The frames of this figure show that high transfer efficiency is possible and that this efficiency has a very marked preference for some combinations of pump and Stokes frequencies.

The narrow ridge indicating very high, and selective, population transfer coincides with the two-photon resonance condition. The width of this narrow feature, where STIRAP takes place, is the two-photon linewidth.

The weaker values of population transfer, forming a shallow background at all detunings, is caused by optical pumping. This mechanism is strongest when the pump is resonant with an intermediate state whose spontaneous emission will populate those final states whose magnetic quantum number differs from the intermediate state by no more than one unit. This mechanism produces the broad ridges, with widths set by the power-broadening of the pump transition.

A set of narrow valleys runs parallel to the sharp STIRAP ridge. These are regions of the plot where STIRAP transfer takes place to other final states. The widths of all the features, both the central ridge and the adjacent valleys, increase with increasing Rabi frequency. This is an example of power broadening.

The STIRAP ridge has one or two distinct notches, where the population transfer drops dramatically. Detailed examination of time histories and dressed state components have revealed several causes for such failures of population transfer. In some cases there occurs a failure of the initial state to connect adiabatically to the desired final state and population merely returns to the initial state after the pulse sequence concludes. Other failures are due to a violation of the adiabatic criterion. This need not prevent population transfer because it is sometimes possible to move population diabatically. This is further discussed in Sec. V and, in particular, in the following paper [49].

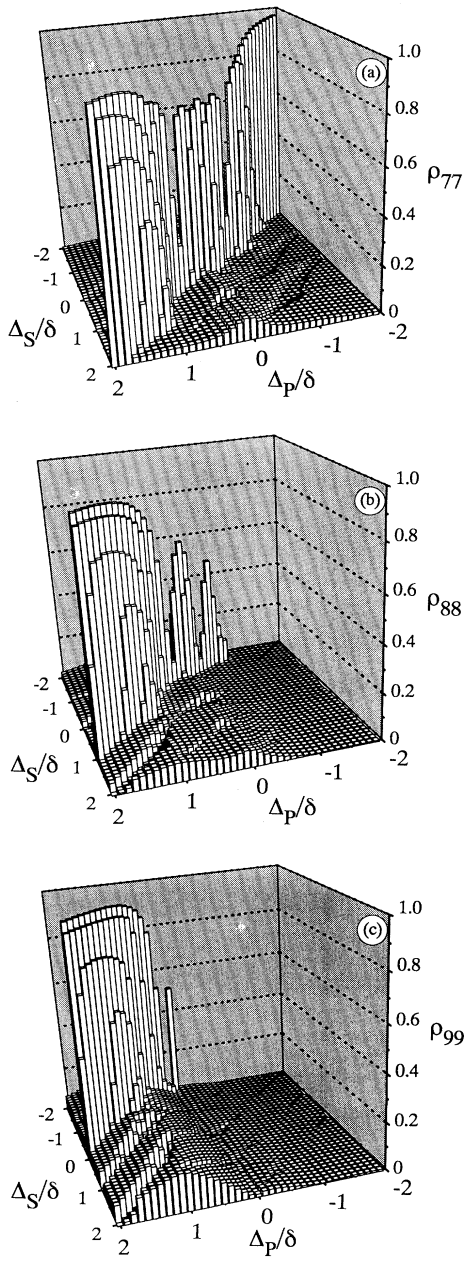

FIG. 16. Population reaching levels (a) 7, (b) 8, and (c) 9 as a function of detuning of the Stokes laser and the pump laser for $\beta_P = 1.31$ rad and $\beta_S = 0.785$ rad. Other relevant parameters are given in Table I.

D. Dependence on Rabi frequency

Although the choice of polarizations and frequencies are the most critical decisions to be made, population

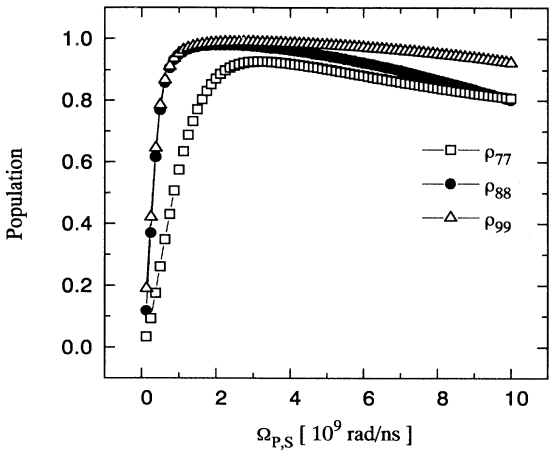

FIG. 17. Population reaching states 7,8,9 ($M = 0, -1, -2$) versus the peak value of Rabi frequencies $\Omega_P^{\max} = \Omega_S^{\max}$. $\Delta_P = 3.14$ rad/ns and the Stokes laser frequency is tuned to match the two-photon resonance with the desired sublevel. The polarization angles are $\beta_P = 1.31$ rad and $\beta_S = 0.785$ rad. The other values of parameters are those given in Table I.

transfer also is affected by the strength of the pulses, as expressed by the peak Rabi frequencies. Figure 17 presents an example of population transfer into states 7–9. Population transfer increases with increasing Rabi frequency, until complete transfer occurs. Population transfer reaches a maximum for peak Rabi frequencies around 2 rad/ns. A further increase in pulse strength causes a decline in this population. Due to increased nonadiabatic coupling more population is placed into excited states, from which it is lost by spontaneous emission.

V. DISCUSSION AND CONCLUSIONS

A. Discussion

We have carried out computer simulations of pulsed excitation by solving the equations of coherent excitation for the populations subject to simplified pulses. We employ both the time-dependent Schrödinger equation and, to include spontaneous emission, the density matrix. From these results, and others reported in [49], we conclude that it is possible to produce highly selective population transfer into selected Zeeman-shifted magnetic sublevels, using a generalization of the STIRAP mechanism. However, a magnetic sublevel structure, usually present, must be considered. When spontaneous emission is negligible, there exist many parameter choices (polarizations and detunings) that can produce complete population transfer. Many of these involve transient population in intermediate states. It is important to recognize that these may fail to be effective choices when spontaneous emission becomes significant because loss and optical pumping can ruin the transfer efficiency.

We have discussed various goals for population transfer by a generalized STIRAP procedure and a number of problems that can occur when implementing the procedures. The magnetic sublevel structure leads to complications of the simple STIRAP concept because multilevel linkages occur, involving branching and competition between possible transfer paths. Consequently, there occur many opportunities for crossings and near crossings of adiabatic eigenvalues. These have important effects.

B. Some specific findings

Our specific findings [52] include the following. The simple choice of polarizations $\beta_P = 0$ and $\beta_S \neq 0$, which might appear to be a natural choice, turns out not to be the best choice for transfering population to large M values. This choice provides direct coupling from the initial state into only one excited sublevel $M = 0$. Transfer of population into $M = 1$ proceeds with one further photon, but transfer into $M = 2$, though possible, requires a three-photon step, entailing a higher Rabi frequency than is required with other polarization choices. We can always choose directions of linear polarization so that there is at all times an adiabatic state with null eigenvalue and no component of population in any excited magnetic sublevel.

If there is a two-photon resonance to state 7 and there is a one-photon resonance between states 1 and 3, then state 3 is a dark state but the adjacent sublevels are transiently populated. This is a consequence of having nonzero linkages to other final states, i.e., the nonresonant pathways influence the dynamics. The population in any of the excited sublevels is subject to loss by spontaneous decay and may thereby prevent complete population transfer. This transient population occurs with greatest probability when the pump field is resonant with state 3 and so it can be reduced by avoiding a one-photon resonance of the pump transition. This loss of transfer efficiency has been observed, but not yet reported in the published literature; see [53].

C. Key issues for STIRAP

We have identified the following four key issues that must be considered when attempting multistate population transfer by counterintuitive pulse sequences (and there are more than three states involved in the linkage).

(1) Initial projection. When the pump pulse is absent, initially, there must be a single adiabatic dressed state that coincides with the initial atomic state. There may be a problem if the null eigenvalue remains degenerate when the Stokes pulse is applied.

(2) Adiabaticity. The system should remain in a single adiabatic state. This requirement has been clarified for conventional STIRAP (i.e., eigenvalues must remain well separated). Multistate systems introduce multiple adiabatic eigenvalues and the interplay between these can become quite complicated, often with near degeneracies and curve crossings occurring. Efficient population transfer may take place even when nonadiabatic evolution occurs, so that examination of adiabatic energy curves does

not always give a clear prediction of success or failure of population transfer.

(3) Connectivity. When the Stokes pulse is absent, toward the conclusion of the counterintuitive pulse sequence, the adiabatic state of interest should coincide with the desired final state. The existence of a nondegenerate zero eigenvalue when only one laser is present does not guarantee the required adiabatic connection. There may be null eigenvalue degeneracies, but these are not detrimental.

(4) Darkness. The adiabatic dressed state that connects to initial and final atomic states should have a negligible component of any intermediate sublevel. This condition holds for conventional three-state STIRAP, but may prove unavailable for more general cases. This fourth condition must be satisfied if the rate of spontaneous emission is appreciable. For the cases treated here, of $J = 0$ to 1 to 2, it is always possible to ensure the existence of a maximally dark state by suitable choice of polarizations. (We shall discuss this further in the following paper [49].)

D. Cautions

For successful population transfer, two-photon resonance is needed, but does not by itself guarantee success. Unlike the case of three-state STIRAP, one-photon resonance may be detrimental to population transfer because it may place transient population into levels subject to spontaneous decay. There occur other poor choices for laser frequencies, not directly related to one-photon resonances, that fail to give population transfer.

Population transfer success depends, sometimes in a subtle way, on polarization angles, Zeeman splitting, and laser detuning. This is because the linkage structure of the Hamiltonian creates many radiation-induced couplings between adiabatic eigenvalues, exhibited as near degeneracies and curve crossings.

We have found situations where, despite making apparently reasonable choices for all the parameters, population fails to transfer. For example, when there is a two-photon resonance to state 7, no one-photon resonance (to minimize detrimental optical pumping), a possible adiabatic connection between desired initial and final states, and the polarization angles have been chosen to ensure a completely dark state at all times, then application of counterpropagating pulses may fail to place any population into the expected final state.

Several things may be occurring to cause such unexpected failure. The interplay among adiabatic eigenvalues may prevent an adiabatic connection of the initial and the final states.

We have also found cases where population transfer succeeds, even though there is no adiabatic connection. The crossings of eigenvalues may be such that transfer through the crossing is diabatic. In this situation the transfer works, although adiabatic considerations would predict failure [49].

E. Recommendations

The choice of experimental conditions (laser polarizations and frequencies) depends on the objectives of the generalized STIRAP process. If the goal is to transfer the highest possible fraction of atoms from an initial state to a single excited state, irrespective of magnetic sublevels, then it is best to choose polarizations that break the multilevel system into separate three-level subsystems. This occurs with parallel linear polarizations of the radiation fields (any magnetic field must be aligned in this same direction). Then one has conventional three-state STIRAP, with no population in radiatively decaying sublevels.

We have here stressed an alternative objective: to transfer the highest possible fraction into a specific magnetic sublevel. Then it is desirable, if possible, to reduce the number of coherently coupled sublevels by starting from $J = 0$. One should choose polarization states of the light that will provide optimum excitation linkages. However, one may wish to study the orientation dependence of a collision process. In such cases one may wish to vary the final magnetic sublevel, during the course of consecutive experimental runs, by using linearly polarized light in a fixed geometry and varying the frequency of one laser. We have demonstrated how this can be done. It is desirable to establish the most general linkage pattern, one which connects all sublevels via a succession of single-photon transitions. The problems that arise in meeting this objective are the main concerns of the present work.

F. Conclusion

Coherent population transfer based on counterintuitive pulse sequences and a generalized STIRAP procedure has, once again, proven to be a powerful and versatile technique. When applied to multilevel problems, successful population transfer is only guaranteed after careful analysis of the situation and proper choice of experimentally controllable parameters.

ACKNOWLEDGMENTS

This work was supported by the Deutsche Forschungsgemeinschaft by the Universität Kaiserslautern Graduierten Kolleg "Laser und Teilchen Spektroskopie," and by a NATO Collaborative Research Grant. The work of B.W.S. is supported in part under the auspices of the U.S. Department of Energy at Lawrence Livermore National Laboratory under Contract No. W-7405-Eng-48. M.P.F. warmly thanks members of the Fachbereich Physik der Universität Kaiserslautern for their hospitality during his period of study leave.

APPENDIX: RWA MATRIX ELEMENTS

For general polarization the coupling coefficients K_{ij} can be constructed via the following steps.

(i) Choose a convenient reference frame for the electric field vector (the polarization direction) of the pump field and a frame for the Stokes field. These frames need not coincide.

(ii) Express the electric field vectors, in their own reference frames, as linear combinations of unit spherical vectors, corresponding either to a single linear polarization vector or to a pair of circularly polarized unit vectors (the helicity basis).

(iii) Use rotation matrices (of order 1) to express these radiation-frame basis vectors in terms of spherical unit vectors in the reference frame defined by the static magnetic field. This is also the reference frame for the angular momentum states of the atom.

(iv) The rotated spherical unit vectors give rotated components of the dipole transition operator. Take matrix elements of these between atomic states. Application of the Wigner-Eckert theorem [11,51] gives a $3j$ symbol and the coordinate transformation gives a rotation matrix element. The product of these, when multiplied by an electric field amplitude, is a Rabi frequency appropriate to a particular sublevel transition.

Following this approach, we obtain the matrix elements of the electric dipole interaction in an angular momentum basis, expressed as Rabi frequencies [50,51]. For the $1 \Leftrightarrow 2$ transition the matrix element is

$$\hbar\Omega(J_1M_1;J_2M_2) = -\mathcal{E}_P^* \sum_q (-1)^q \epsilon_q \langle J_1M_1|d_{-q}|J_2M_2\rangle. \quad \text{(A1)}$$

A comparable formula applies to the $2 \Leftrightarrow 3$ transition, but with the replacement of the complex-valued envelope $\mathcal{E}_P^*$ with $\mathcal{E}_S$. We extract the dependence upon magnetic quantum numbers into a 3-j symbol by employing the Wigner-Eckart theorem to write

$$\hbar\Omega(J_1M_1;J_2M_2) = -\mathcal{E}_P^*(J_1||d||J_2) \times \sum_q \epsilon_q (-1)^{J_1-M_1+q} \begin{pmatrix} J_1 & 1 & J_2 \\ -M_1 & q & M_2 \end{pmatrix}. \quad \text{(A2)}$$

The prefactor to this summation represents a root mean square Rabi frequency, averaged over the dipole orientation and the magnetic sublevels. The reduced dipole matrix element $(J_1||d||J_2)$ that occurs here also occurs in such spectroscopic observables as oscillator strengths and Einstein A coefficients. The connection with the latter, for example, is (see [11], p. 1353)

$$|\overline{\Omega_{ij}}|^2 = |\mathcal{E}(J_i||d||J_j)/\hbar|^2 = \frac{\lambda^3}{4\pi^2\hbar c} I g_i A_{ij}, \quad \text{(A3)}$$

where I is the instantaneous irradiance (power per unit area) and g_i is the statistical weight of the upper level.

[1] U. Gaubatz, P. Rudecki, M. Becker, S. Schiemann, M. Külz, and K. Bergmann, Chem. Phys. Lett. **149**, 463 (1988).

[2] K. Bergmann, in *Atomic and Molecular Beam Methods*, edited by G. Scoles (Oxford University Press, Oxford, 1988), pp. 293–344.

[3] U. Gaubatz, P. Rudecki, S. Schiemann, and K. Bergmann, J. Chem. Phys. **92**, 5363 (1990).

[4] H.-G. Rubahn and K. Bergmann, Annu. Rev. Phys. Chem. **41**, 735 (1990).

[5] N. Dam, L. Oudejans, and J. Reuss, Chem. Phys. **140**, 217 (1990).

[6] C. Liedenbaum, S. Stolte, and J. Reuss, Phys. Rep. **178**, 1 (1989).

[7] P. Brumer and M. Shapiro, Annu. Rev. Phys. Chem. **43**, 257 (1992).

[8] P. Marte, P. Zoller, and J. L. Hall, Phys. Rev. A **44**, R4118 (1991).

[9] B. Broers, H. B. van Linden van den Heuvell, and L. D. Noordam, Phys. Rev. Lett. **69**, 2062 (1992).

[10] S. Schiemann, A. Kuhn, S. Steuerwald, and K. Bergmann, Phys. Rev. Lett. **71**, 3637 (1993).

[11] B. W. Shore, *The Theory of Coherent Atomic Excitation* (Wiley, New York, 1990).

[12] X. Yang and A. M. Wodtke, J. Chem. Phys. **92**, 116 (1990).

[13] P. Dittmann, F. P. Pesl, J. Martin, G. W. Coulston, G. Z. He, and K. Bergmann, J. Chem. Phys **98**, 9472 (1992).

[14] M. Külz, A. Kortyna, M. Keil, B. Schellhaaß, and K. Bergmann (unpublished).

[15] R. Sussmann, R. Neuhauser, and H. J. Neusser, J. Chem. Phys. **100**, 4784 (1994).

[16] A. S. Parkins, P. Marte, P. Zoller, and H. J. Kimble, Phys. Rev. Lett. **71**, 3095 (1993).

[17] K. Bergmann, U. Hefter, and J. Witt, J. Chem. Phys. **72**, 4777 (1980).

[18] M. Fuchs and J. P. Toennies, J. Chem. Phys. **85**, 7062 (1986).

[19] C. E. Hamilton, J. L. Kinsey, and R. W. Field, Annu. Rev. Phys. Chem. **37**, 493 (1986).

[20] *Molecular Dynamics and Spectroscopy by Stimulated Emission Pumping*, edited by H. C. Dai and R. W. Field (World Scientific, Singapore, 1995).

[21] L. Allen and J. H. Eberly, *Optical Resonance and Two-Level Atoms* (Wiley, New York, 1975).

[22] J. S. Melinger, S. R. Gandhi, A. Hariharan, J. X. Tull, and W. S. Warren, Phys. Rev. Lett. **68**, 2000 (1992); J. S. Melinger, S. R. Gandhi, A. Hariharan, D. Goswami, and W. S. Warren, J. Chem. Phys. **101**, 6439 (1994).

[23] K. Bergmann and B. W. Shore, in *Molecular Dynamics and Spectroscopy by Stimulated Emission Pumping* (Ref. [20]), Chap. 9.

[24] B. W. Shore, K. Bergmann, and J. Oreg, Z. Phys. D **23**, 33 (1992).

[25] Y. B. Band and P. S. Julienne, J. Chem. Phys. **94**, 5291 (1991).
[26] Y. B. Band and P. S. Julienne, J. Chem. Phys. **95**, 5681 (1991).
[27] Y. B. Band and P. S. Julienne, J. Chem. Phys. **97**, 9107 (1992).
[28] G. Coulston and K. Bergmann, J. Chem. Phys. **96**, 3467 (1992).
[29] G. Z. He, A. Kuhn, S. Schiemann, and K. Bergmann, Opt. Soc. Am. B **7**, 1960 (1990).
[30] F. T. Hioe and J. H. Eberly, Phys. Rev. Lett. **47**, 838 (1981).
[31] F. T. Hioe, Phys. Lett. **99A**, 150 (1983).
[32] F. T. Hioe and C. E. Carroll, Phys. Rev. A **37**, 3000 (1988).
[33] A. Kuhn, G. Coulston, G. Z. He, S. Schiemann, K. Bergmann, and W. S. Warren, J. Chem. Phys. **96**, 4215 (1992).
[34] J. R. Kuklinski, U. Gaubatz, F. T. Hioe and K. Bergmann, Phys. Rev. A **40**, 6741 (1989).
[35] J. Oreg, F. T. Hioe, and J. H. Eberly, Phys. Rev. A **29**, 690 (1984).
[36] J. Oreg, G. Hazak, and J. H. Eberly, Phys. Rev. A **32**, 2776 (1985).
[37] J. Oreg, K. Bergmann, B. W. Shore, and S. Rosenwaks, Phys. Rev. A **45**, 4888 (1992).
[38] B. W. Shore, K. Bergmann, J. Oreg, and S. Rosenwaks, Phys. Rev A **44**, 7442 (1991).
[39] B. W. Shore, K. Bergmann, A. Kuhn, S. Schiemann, J. Oreg, and J. H. Eberly, Phys. Rev. A **45**, 5297 (1992).
[40] H.-G. Rubahn, E. Konz, S. Schiemann, and K. Bergmann, Z. Phys. D **22**, 401 (1991).
[41] A. V. Smith, J. Opt. Soc. Am. B **9**, 1543 (1992).
[42] W. Bussert, T. Bregel, R. J. Allan, M.-W. Ruf, and H. Hotop, Z. Phys. A **320**, 105 (1985).
[43] W. Bussert, Z. Phys. D **1**, 321 (1986).
[44] U. Hefter, G. Ziegler, A. Mattheus, A. Fischer, and K. Bergmann, J. Chem. Phys. **85**, 286 (1986).
[45] A. Mattheus, A. Fischer, G. Ziegler, E. Gottwald, and K. Bergmann, Phys. Rev. Lett. **56**, 712 (1986).
[46] L. S. Goldner, C. Gerz, R. J. Spreeuw, S. L. Rolston, C. I. Westbrook, W. D. Phillips, P. Marte, and P. Zoller, Phys. Rev. Lett. **72**, 997 (1994).
[47] J. Lawall and M. Prentiss, Phys. Rev. Lett. **72**, 993 (1994).
[48] P. Pillet, C. Valentin, R.-L. Yuan, and J. Yu, Phys. Rev. A **48**, 845 (1993).
[49] J. Martin, B. W. Shore, and K. Bergmann, following paper, Phys. Rev. A **52**, 583 (1995).
[50] M. P. Fewell, J. Phys. B **26**, 1957 (1993).
[51] R. N. Zare, *Angular Momentum: Understanding Spatial Aspects in Chemistry and Physics* (Wiley, New York, 1988).
[52] J. Martin, Ph.D. thesis, Universität Kaiserslautern, 1995 (unpublished).
[53] A. Kuhn, *Diplomarbeit*, Universität Kaiserslautern, 1990 (unpublished); E. Konz, *Diplomarbeit*, Universität Kaiserslautern, 1991 (unpublished); M. Verbeck, *Diplomarbeit*, Max-Planck Institut für Strömungsforschung, Göttingen, 1994 (unpublished).

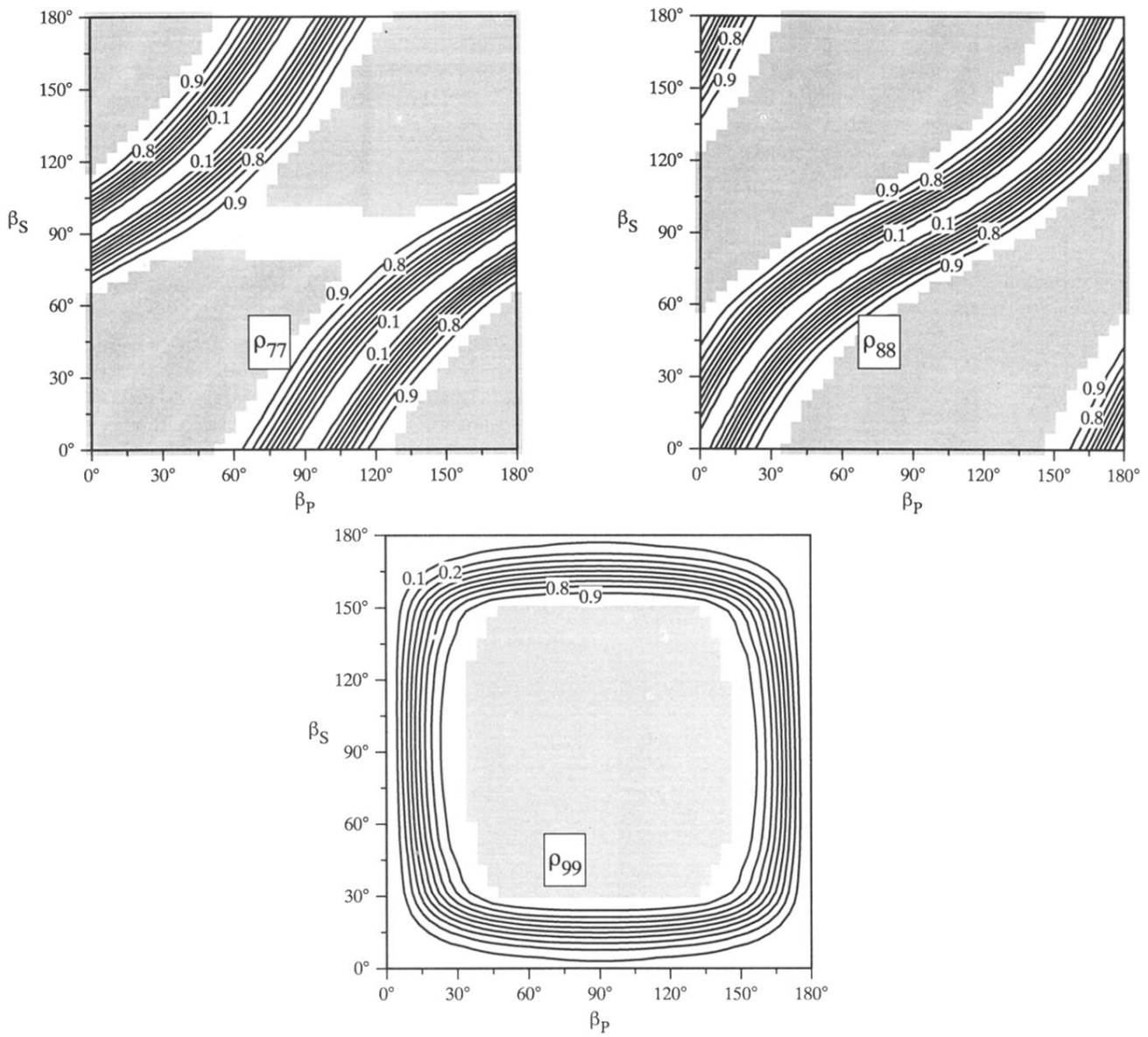

FIG. 13. Contour plots of populations reaching selected final states, as a function of pump polarization angle and Stokes polarization angle. The pump field is not resonant ($\Delta_P = 6.28$ rad/ns). Selected final states are $M = 0$ (state 7, upper frame), $M = +1$ (state 8, center frame), and $M = +2$ (state 9, lower frame). Regions where transfer efficiency exceeds 95% are gray. The parameters are given in Table I. In each case the Stokes laser frequency is chosen to establish the appropriate two-photon resonance condition.

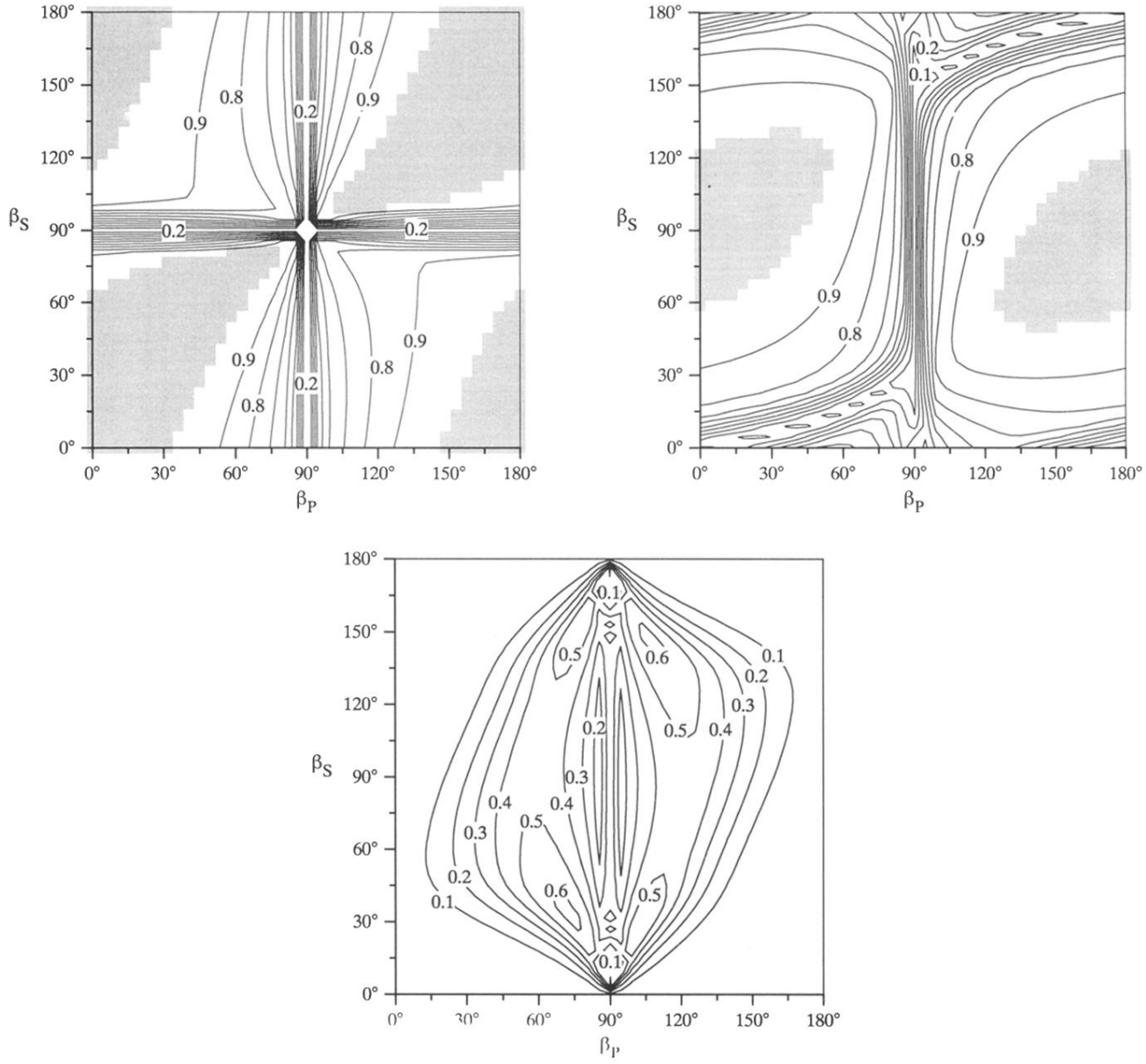

FIG. 14. Same as in Fig. 13 but the pump field is resonant with state 3 ($M = 0$).

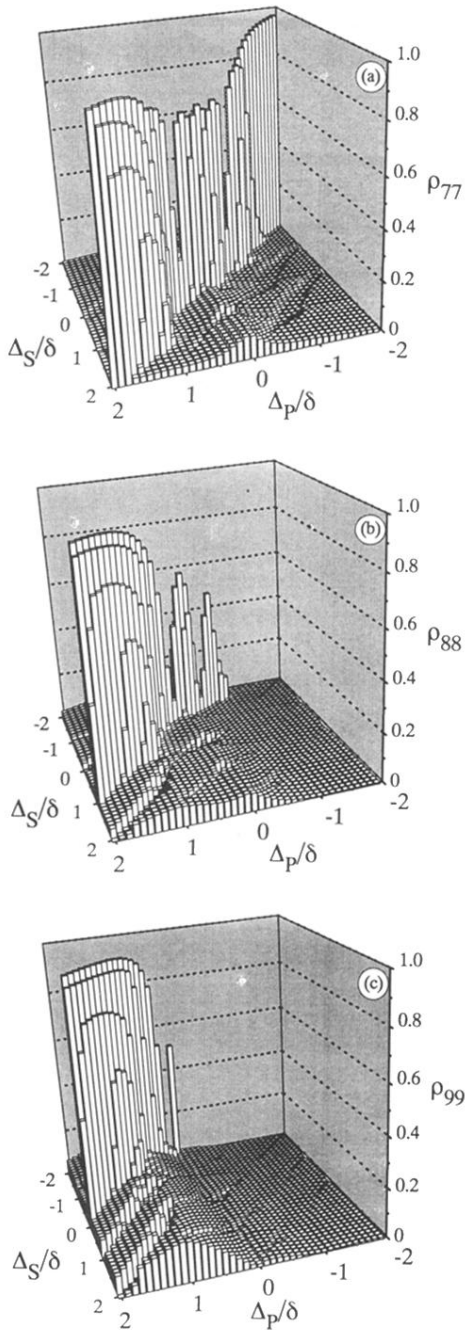

FIG. 16. Population reaching levels (a) 7, (b) 8, and (c) 9 as a function of detuning of the Stokes laser and the pump laser for $\beta_P = 1.31$ rad and $\beta_S = 0.785$ rad. Other relevant parameters are given in Table I.